IEEE Access
Multidisciplinary | Rapid Review | Open Access Journal

Received February 23, 2020, accepted February 27, 2020, date of publication March 2, 2020, date of current version March 16, 2020.

Digital Object Identifier 10.1109/ACCESS.2020.2977609

Adaptive Sliding Mode Control Design for Nonlinear Unmanned Surface Vessel Using RBFNN and Disturbance-Observer

ZHENG CHEN[1,2], (Senior Member, IEEE), YOUGONG ZHANG[2], YONG NIE[1], JIANZHONG TANG[1], AND SHIQIANG ZHU[2,3]

[1]The State Key Laboratory of Fluid Power and Mechatronic Systems, Zhejiang University, Hangzhou 310027, China
[2]Ocean College, Zhejiang University, Zhoushan 316021, China
[3]Zhejiang Laboratory, Hangzhou 311100, China

Corresponding author: Yong Nie (ynie@zju.edu.cn)

This work was supported in part by the Natural Science Foundation of Zhejiang Province, China, under Grant LY19E050016, in part by the National Natural Science Foundation of China under Grant 61603332, and in part by the Fundamental Research Funds for the Central Universities.

ABSTRACT Unmanned surface vessel(USV) has been applied in the maritime security inspection and resources exploration to execute complex works with its advantages in automation and intelligence. While the nonlinear USV working in the complex ocean environment, the good trajectory tracking performance is an important capacity. However, the nonlinearity, modeling uncertainties (e.g., modeling error and parameter variations) and external disturbance (wind, wave, current, etc) are the main difficulties, which deteriorates the control performance. To solve this issue, most existing algorithms for USV's tracking have been developed based on the linearization of the USV's nonlinear dynamic model at specific equilibrium point. However, the integrated effect of nonlinearities, modeling uncertainties and external disturbance has not been well considered, which can degrade the USV's tracking performance. Therefore, to achieve the good tracking performance for USV, a nonlinear dynamic model is strictly derived in this paper with the integrate consideration of abovementioned issues, and an adaptive sliding mode control design using RBFNN(Radial Basis Function Neural Network) and disturbance-observer is subsequently developed, where a RBFNN approximator is designed to approximate and compensate modeling uncertainties, and a disturbance-observer is designed to estimate and compensate the effect of the external disturbance. Furthermore, the global stability of the overall closed-loop system of USV are strictly guaranteed. The comparative simulation is carried out to validate the fast response, better transient performance and robustness of our proposed control design via comparing with the existing methods.

INDEX TERMS Adaptive sliding mode control, neural network, unmanned surface vessel(USV), Lyapunov stability theorem, disturbance observer.

I. INTRODUCTION

With the development of advanced mechatronics and automation [1]–[4], unmanned surface vessel(USV) can undertake the oceanic tasks with the advantages of intelligence and safety, and has been widely applied in military and commercial fields in a long time [5]–[9], such as oceanic exploration and collection, maritime rescue, environmental inspection, etc. While the USV working in the complex ocean environment, the nonlinearity, modeling uncertainties which consist of(e.g., modeling error and parameter variations) and external disturbance (wind, wave, current, etc) are the main difficulties, which deteriorates the control performance [10], [11], thus the accurate trajectory tracking is still a challenge for the USV's control.

To improve the USV's trajectory tracking performance, several control algorithms have been developed based on the linearization of the USV's nonlinear dynamic model at specific equilibrium point, which has good performance for trajectory tracking around the specific equilibrium point.

The associate editor coordinating the review of this manuscript and approving it for publication was Jun Hu.

For instance, to solve the uncertainties and time-varying disturbances, an adaptive course control algorithm was proposed by Qiu *et al*. [12] based on trajectory linearization control technology, where a finite-time disturbances observer was designed by Wang *et al*. [13] to estimate the external disturbances and sideslip angle which can effect the USV's tracking performance. To estimate the unmodeled dynamics and disturbances, a fuzzy observer is developed in [14]. Moreover, to solve the matched and unmatched uncertainties, an adaptive control algorithm for the USV's tracking is proposed by Shin *et al*. [15] based on linear dynamic model using dynamic surface and virtual control. Though these control algorithms have been applied in the USV's trajectory tracking, they are not suitable for any desired complex trajectories and only suitable for specific desired trajectories at the equilibrium point. Besides, the modeling uncertainties and external disturbance are not well considered in the aforementioned linear controller, thus a more suitable trajectory tracking controller based on the nonlinear USV's dynamics with integrate consideration of the nonlinearity, modeling uncertainties and external disturbances is still a challenge to be developed.

For the USV's trajectory tracking with complex external disturbances, some trajectory control algorithms have been proposed based on nonlinear dynamic model [16]–[23], such as adaptive back-stepping control, sliding mode control, neural network-based control, model predictive control, etc. For instance, to achieve the good tracking performance, a disturbance-observer-based sliding mode control design is proposed in [16], where a disturbance observer is designed to estimate and compensate the modeling uncertainties and external disturbance. A nonlinear modeling scheme based on active Kalman filter was proposed by Han *et al*. [24] to estimate and compensate the unstructured model. An adaptive trajectory tracking control algorithm was proposed by Chen *et al*. [25]. It is worth mentioning that neural networks is designed in this paper to estimate the USV's hydrodynamics and external disturbances, and an observer is used to observe the unmeasurable velocities of output feedback controller. To deal with the saturation and constraints of USV's actuator and yaw, Guo and Zhang [26] proposed a tracking control algorithm using back-stepping control method, where an observer is derived to observe the USV's actuator dead-zones and disturbances. Moreover, a model-based event-triggered control method is proposed by Deng *et al*. [27], where a neural networks approximator is designed to estimate uncertainties from both internal system and external environment. To process the external environment disturbances, a control scheme based on model predictive method is proposed by Tan *et al*. [28] with the consideration of USV's physical constraints, which can be calculated and implemented online. To improve the tracking performance and robustness, a control strategy with the integrate consideration of port-controlled hamiltonian method and back-stepping method is proposed by Lv *et al*. [29], which provides the experience to develop the comprehensive application of multiple control methods.

Though several control algorithms have been tried to achieve better performance, few algorithms can take full account of the integrated challenges consist of the USV's nonlinearities, modeling uncertainties and external disturbance. Therefore, good tracking performance is still challenging to be developed for USV's control. In this paper, an adaptive sliding mode control algorithm using RBFNN and disturbance-observer is proposed based on nonlinear USV's dynamic model. The main works and improvements over the existing methods can be listed as follows:

(a) A nonlinear dynamic model for USV is established, where the modeling uncertainties and external disturbances are fully taken into account.

(b) The modeling uncertainties are related with the motion state and dynamic parameters of the USV. To approximate and compensate modeling uncertainties, a RBFNN approximator is designed with its characteristic of universal approximation.

(c) Considering that the time-varying external disturbance is caused by the wind, wave and current, a disturbance observer is designed in this paper to observe and then compensate it.

(d) Integrating the RBFNN approximation and disturbance-observer, an adaptive sliding mode algorithm is developed for USV's nonlinear dynamics, which is more suitable for any desired trajectories.

Therefore, the integrate effect of system nonlinearity, modeling uncertainties and external disturbance of the USV can be well handled using RBFNN and disturbance-observer. Furthermore, to verify the effectiveness and priority of our proposed control design, the comparative simulations with different controllers and different desired trajectories are implemented, which shows the faster response, better transient and robustness of proposed control design.

The structure of this paper is roughly described as follows. Section II mainly describes the framework of the RBFNN and the definition of related physical parameter. With full consideration of modeling uncertainties and external disturbances, the modeling of the USV is derived in Section III. Subsequently, Section IV mainly describes the design of the adaptive slide-mode controller using RBFNN and disturbance observer. To prove the stability of the overall closed-loop system, the related derivation is also described in Section IV. Moreover, Section V presents the simulation of USV's tracking with different control algorithms and different desired trajectories, which verifies the significant tracking priority of proposed control design. Finally, the contributions and future research are summarized in Section VI.

II. THE DEFINITION OF RBFNN

Due to the advantages of universal approximation [30], the RBFNN algorithm has been widely applied for the model-uncertain systems. Moreover, the framework of the RBFNN and its definition can be described as follows in detail:

Definition 1 : As a kind of forward neural network, RBFNN consists of input layer, hidden layer and output layer,

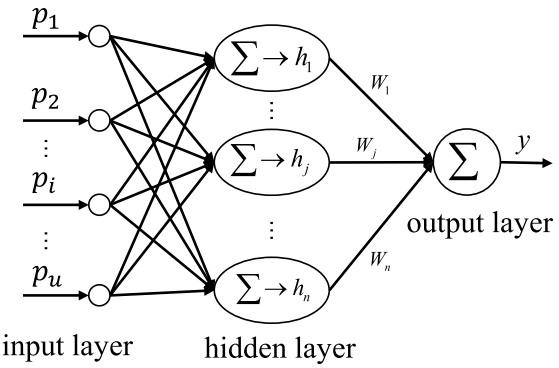

FIGURE 1. The framework of RBFNN.

the detailed framework is shown in Fig.1, where u and n represent the number of node in input layer and hidden layer respectively.

The input function of RBFNN can be listed as:

$$p = [p_1, \ldots, p_i, \ldots, p_u]^T \tag{1}$$

Then the Gaussian function can be described as:

$$h_j(p) = \exp\left(-\frac{\|p - c_j\|^2}{b_j^2}\right) \tag{2}$$

$$h(p) = \left[h_1(p), \ldots, h_j(p), \ldots, h_n(p)\right]^T \tag{3}$$

where $\|\bullet\|$ represents the Euclidean norm of $\bullet$, $j = 1, \ldots, n$, $c_j = \left[c_{j1}, \ldots, c_{ji}, \ldots, c_{ju}\right]^T$. The output function of RBFNN is defined as follows:

$$y = \sum_{j=1}^{n} W_j h_j(p) + \varsigma = W^T h(p) + \varsigma \tag{4}$$

where $W = \left[W_1, \ldots, W_j, \ldots, W_n\right]^T$ represents the output weight of each hidden node, ς is the estimation error.

III. THE MODELING OF USV's OVERALL SYSTEM

A. NONLINEAR MODELING

As a 3-DOF object in the plane, the model of USV is described in Fig.2, and its kinematic model is derived as:

$$\dot{\eta} = R(\psi) V \tag{5}$$

As shown in Fig.2, $\eta = \left[x\ y\ \psi\right]^T$ represents the position vector of USV, where x, y represent the global coordination and ψ represents the heading angle of the USV. $V = \left[u\ v\ r\right]^T$ represents the corresponding velocity state vector, where u, v and r represent the surge, sway velocities and yaw rotational velocity respectively. $R(\psi)$ represents the rotation matrix from body frame $\{b\}$ to ground frame $\{i\}$, which is defined as follows,

$$R(\psi) = \begin{bmatrix} \cos\psi & -\sin\psi & 0 \\ \sin\psi & \cos\psi & 0 \\ 0 & 0 & 1 \end{bmatrix} \tag{6}$$

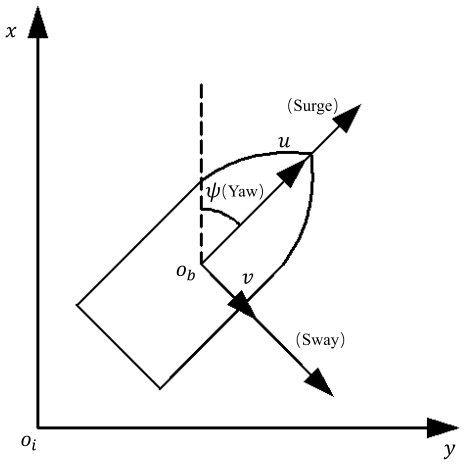

FIGURE 2. The model of USV.

With the integrate consideration of external disturbance and modeling uncertainties, the USV's nonlinear dynamic model is be derived as:

$$M'\dot{V} + C'V + D'V = \tau + R^T d_s \tag{7}$$

where $\tau\left(\left[\tau_x\ \tau_y\ \tau_n\right]^T\right)$ is the USV's control vector. M' is the USV's inertial matrix, which consists of known part M_0' and unknown part $\Delta M'$. The coriolis and centripetal term C' is a skew-symmetric matrix, which consists of known part C_0' and unknown part $\Delta C'$. D' is the damping matrix, which consists of known part D_0' and unknown part $\Delta D'$. d_s represents the USV's external disturbance caused by wind, wave and current, which can be estimated and compensated by disturbance observer in Section IV. The matrices M_0', C_0' and D_0' can be described as follows:

$$M_0' = \begin{bmatrix} m - X_{\dot{u}} & 0 & 0 \\ 0 & m - Y_{\dot{v}} & mx_g - Y_{\dot{r}} \\ 0 & mx_G - N_{\dot{v}} & I_{zz} - N_{\dot{r}} \end{bmatrix} \tag{8}$$

$$C_0' = \begin{bmatrix} 0 & 0 & -m_{22}v - m_{23}r \\ 0 & 0 & m_{11}u \\ m_{22}v + m_{23}r & -m_{11}u & 0 \end{bmatrix} \tag{9}$$

and

$$D_0' = -\begin{bmatrix} X_u & 0 & 0 \\ 0 & Y_v & Y_r \\ 0 & N_v & N_r \end{bmatrix} \tag{10}$$

where m represents the mass of USV. I_{zz} represents the USV's moment of inertia. x_g represents the gravity center's position. X_*, Y_*, Z_* represent hydrodynamic coefficients. m_{ij} represents the element in the row i and column j of M_0'.

As we all know, the driving forces and torque of the USV can be produced by the water-jet propulsion as:

$$\tau = \begin{bmatrix} \tau_x \\ \tau_y \\ \tau_n \end{bmatrix} = \begin{bmatrix} T\cos\delta_r \\ -T\sin\delta_r \\ x_{\delta_r} T\sin\delta_r \end{bmatrix} \tag{11}$$

where T represents driving force produced by the water-jet propulsion, δ_r represents the rudder angle of the water-jet propulsion, the x_{δ_r} represents the install position of the water-jet nozzle.

By substituting (5) to (7), the nonlinear USV system can be derived in the Lagrange form [17]:

$$M_0\ddot{\eta}+C_0\dot{\eta}+D_0\dot{\eta} = R\tau + d_m + d_s \tag{12}$$

where $M_0 = RM_0'R^T$, $C_0 = R\left(C'_0 - M'_0R^T\dot{R}\right)R^T$, $D_0 = RD_0'R^T$, d_m represents various modeling uncertainties (e.g., modeling error and parameter variations), which can be approximated by RBFNN. Some properties and assumptions of (12) can be listed as follows:

Property 1: $\dot{M}_0 - 2C_0$ is skew-symmetric, $\dot{M}_0 - 2C_0 = -\left[\dot{M}_0 - 2C_0\right]^T$.

Assumption 1: The modeling uncertainties d_m is with the upper bound as: $\|d_m\| \le d_m^*$

Assumption 2: While the USV working, it is usually considered that the external disturbances d_s is superimposed by the low frequency period signals [13], and the derivative of d_s is assumed to have an upper bound, which means $\left\|\dot{d}_s\right\| \le d_s'$.

B. LINEAR MODELING

To enhance the trajectory tracking performance of USV, several proposed control algorithms have been proposed based on the linearization of the USV's nonlinear dynamic model at specific equilibrium point. To better analyze the physical meaning of the specific equilibrium point, the derivation process of the linear model is described as follows in detail.

According to [15], the equilibrium point of USV is defined as:

$$u = u_0, v = 0, r = 0, \delta_r = 0, T = T_0 \tag{13}$$

With the abovementioned nonlinear dynamic model (7) and equilibrium point (13), the USV's surge dynamics is derived as:

$$\Delta\dot{u} = a_u\Delta u + b_u\Delta T \tag{14}$$

where $\Delta u = u - u_0$, $\Delta T = T - T_0$, $a_u = \frac{X_u}{m-X_{\dot{u}}}$, $b_u = \frac{1}{m-X_{\dot{u}}}$.

With the Nomoto's steering model [15], the USV's yaw dynamics can be calculated with the following first-order dynamics:

$$\tau_r\Delta\dot{r} + \Delta r = b_r\Delta\delta_r \tag{15}$$

where $b_r = \frac{T_0x_{\delta_r}}{I_{zz}-N_{\dot{r}}}$.

Moreover, assume that u is almost unchanged and the yaw perturbation is small, the USV's sway dynamics can be derived as:

$$\tau_\beta\Delta\dot{\beta} + \Delta\beta = -K_\beta\Delta r \tag{16}$$

where β represents the sideslip angle which can be calculated by $\Delta\beta = atan2\left(\frac{\Delta v}{\Delta u}\right)$.

With the abovementioned surge dynamics (14), yaw dynamics (23), and sway dynamics (16), the linearized dynamic model of USV is summarized as:

$$\dot{x} = Ax + B\delta + \Delta \tag{17}$$

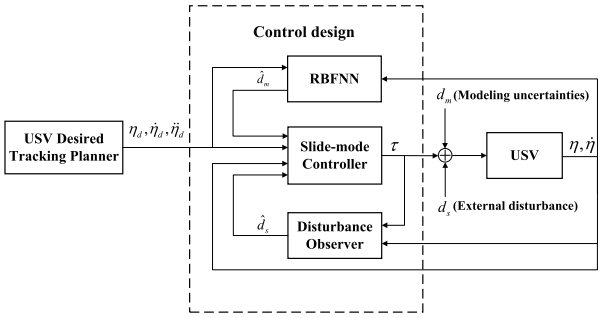

FIGURE 3. Adaptive sliding mode control architecture for nonlinear USV system using RBFNN and disturbance-observer.

where $x = \left[\begin{array}{cccc} u & \beta & \psi & r \end{array}\right]^T$ represents the motion state of USV, $\delta = \left[\begin{array}{cc} T & \delta_r \end{array}\right]^T$ represents the control input,

$$A = \begin{bmatrix} a_u & 0 & 0 & 0 \\ 0 & -\frac{1}{\tau_\beta} & 0 & -\frac{K_\beta}{\tau_\beta} \\ 0 & 0 & 0 & 1 \\ 0 & 0 & 0 & -\frac{1}{\tau_r} \end{bmatrix} \tag{18}$$

$$B = \begin{bmatrix} b_u & 0 \\ 0 & 0 \\ 0 & 0 \\ 0 & \frac{b_r}{\tau_r} \end{bmatrix} \tag{19}$$

With the desired trajectory η_d, $\dot{\eta}_d$ and $\ddot{\eta}_d$ designed by trajectory planner, the control objective for the USV is to track the desired trajectory with faster response, better transient and robustness, where $\eta_d = \left[\begin{array}{ccc} x_d & y_d & \psi_d \end{array}\right]^T$, $\dot{\eta}_d = \left[\begin{array}{ccc} \dot{x}_d & \dot{y}_d & \dot{\psi}_d \end{array}\right]^T$, $\ddot{\eta}_d = \left[\begin{array}{ccc} \ddot{x}_d & \ddot{y}_d & \ddot{\psi}_d \end{array}\right]^T$,

IV. ADAPTIVE SLIDING MODE CONTROL DESIGN USING RBFNN AND DISTURBANCE-OBSERVER

As shown in Fig.3, an adaptive sliding mode controller is proposed using RBFNN and disturbance-observer to track the desired trajectory η_d, $\dot{\eta}_d$, $\ddot{\eta}_d$. A RBFNN approximator is designed to approximate and compensate modeling uncertainties, and a disturbance-observer is designed to estimate and compensate the effect of the external disturbance. Furthermore, the overall stability of the control system is proved.

A. CONTROLLER DESIGN

According to [31]–[34], the sliding-mode surface s can be defined with the tracking errors:

$$s = Ke + \dot{e} \tag{20}$$

where $e = \eta - \eta_d$, $K = diag\{k_1, \ldots, k_i, \ldots, k_w\}$, $i = 1, 2, \ldots, w$.

Substituting (12) into (20), thus,

$$\begin{aligned} M_0\dot{s} &= M_0(\ddot{\eta} - \ddot{\eta}_d + k\dot{e}) \\ &= M_0(k\dot{e} - \ddot{\eta}_d) + M_0\ddot{\eta} \\ &= M_0(k\dot{e} - \ddot{\eta}_d) - C_0\dot{\eta} - D_0\dot{\eta} + R\tau + d_s + d_m \\ &= M_0(k\dot{e} - \ddot{\eta}_d) - C_0(s + \dot{\eta}_d - ke) - D_0\dot{\eta} + R\tau + d_s + d_m \\ &= M_0(k\dot{e} - \ddot{\eta}_d) - C_0(\dot{\eta}_d - ke) - C_0s - D_0\dot{\eta} \\ &\quad + R\tau + d_s + d_m \end{aligned} \tag{21}$$

Then, the adaptive control input τ for the USV can be designed as [35]–[38]:

$$\tau = -R^T \left(\rho + K_v s + \hat{d}_m + \xi sat\,(s) + \hat{d}_s \right) \tag{22}$$

where $\rho = -M_0(\ddot{\eta}_d - k\dot{e}) - C_0(\dot{\eta}_d - ke) - D_0\dot{\eta}$. $\hat{d}_s$ represent the estimate value of the disturbance observer. $sat(s)$ is a saturation function to avoid the chattering phenomenon, which is designed as:

$$sat(s) = \begin{cases} 1 & s > \Delta \\ \dfrac{1}{\Delta} s & \|s\| \le \Delta \\ -1 & s < -\Delta \end{cases} \tag{23}$$

, Δ is the positive boundary layer, which can be selected as: $\Delta = \frac{4\varepsilon}{\xi}$.

$\hat{d}_m$ represent the output value of the RBFNN to approximate the unknown nonlinear modeling uncertainties d_m, which can be designed as follows:

$$\hat{d}_m = \hat{W} h\,(p) \tag{24}$$

where

$$p = [\dot{\eta}_d, \dot{e}, \eta_d, e] \tag{25}$$

$$h_j(p) = \exp\left(-\frac{||p - c_j||^2}{b_j^2} \right) \tag{26}$$

$$h(p) = [h_j(p)]^T \tag{27}$$

$$d_m = Wh(p) + \varsigma \tag{28}$$

where ς is the estimate error of RBFNN with the upper bound:

$$\|\varsigma\| \le \varsigma^* \tag{29}$$

The adaptive law of RBFNN can be designed as:

$$\dot{\hat{W}} = \frac{1}{\delta} sh(p) \tag{30}$$

where δ is the positive parameter of the adaptive law.

B. DISTURBANCE-OBSERVER DESIGN

To estimate and compensate the USV's external disturbance caused by wind, wave and current, the disturbance observer $\hat{d}_s$ is designed with the following equation:

$$\begin{aligned} \dot{Z} &= L\,(C_0\dot{\eta} + D_0\dot{\eta} - R\tau) - L\hat{d}_s \\ \hat{d}_s &= Z + P \end{aligned} \tag{31}$$

where,

$$L = H^{-1} M_0^{-1} \tag{32}$$

$$P = H^{-1}\dot{\eta} \tag{33}$$

H is a invertible constant matrix, and can be selected according to the transient and steady-state response of disturbance observer. Moreover, M_0 and L are a constant. Therefore, the derivative of P is derived with (32) and (33):

$$\dot{P} = LM_0\ddot{\eta} \tag{34}$$

As $\tilde{d}_s = d_s - \hat{d}_s$ represent the estimate error, the derivative of $\tilde{d}_s$ can be derived as the following equation:

$$\begin{aligned} \dot{\tilde{d}}_s &= \dot{d}_s - \dot{\hat{d}}_s \\ &= \dot{d}_s - \dot{Z} - \dot{P} \\ &= \dot{d}_s - L\,(C_0\dot{\eta} + D_0\dot{\eta} - R\tau) + L\hat{d}_s - LM_0\ddot{\eta} \\ &= \dot{d}_s + L\hat{d}_s - L\,(M_0\ddot{\eta} + C_0\dot{\eta} + D_0\dot{\eta} - R\tau) \\ &= \dot{d}_s + L\hat{d}_s - L\,(d_s + d_m) \\ &= \dot{d}_s - L\tilde{d}_s - Ld_m \\ &= -L\tilde{d}_s + \mu \end{aligned} \tag{35}$$

where $\mu = \dot{d}_s - Ld_m$, which is bounded since $\dot{d}_s$ and d_m are bounded with assumption 1 and 2. It follows that:

$$\tilde{d}_s \le e^{-Lt}\tilde{d}_s\,(0) + \frac{\mu}{L}\left(1 - e^{-Lt}\right) \tag{36}$$

Thus, the observer error $\tilde{d}_s$ is bounded as $t \to \infty$, which reflects stability of disturbance observer (31) with bounded-input bounded-output stability.

C. OVERALL STABILITY ANALYSIS

Considering the closed-loop USV control system, one theorem can be listed in the following to verify the overall stability.

Theorem: With the controller (22), RBFNN approximator (24) and disturbance observer (31), the modeling uncertainties and external disturbances can be well estimated and compensated and the overall control system is stable, all the signals are bounded.

Proof : Considering the overall closed-loop system, define the Lyapunov Function V as:

$$V = \frac{1}{2} sM_0 s + \frac{1}{2}\delta\tilde{W}^T\tilde{W} \tag{37}$$

where $\tilde{W} = W - \hat{W}$. Then, the derivative of V is derived as the following equation.

$$\dot{V} = s^T M_0\dot{s} + \frac{1}{2} s\dot{M}_0 s + \delta\tilde{W}^T\dot{\tilde{W}} \tag{38}$$

For

$$M_0\dot{s} = d_m - K_v s - \hat{d}_m - \xi sat\,(s) - \hat{d}_s - C_0 s + d_s \tag{39}$$

Substituting (39) and (22) into (38), then,

$$\begin{aligned} \dot{V} &= s^T \left(d_m - K_v s - \hat{d}_m - \xi sat\,(s) - \hat{d}_s - C_0 s + d_s \right) \\ &\quad + \frac{1}{2} s\dot{M}_0 s + \delta\tilde{W}^T\dot{\tilde{W}} \\ &= s^T \left(\tilde{d}_m - K_v s - \xi sat\,(s) + \tilde{d}_s \right) \\ &\quad + \frac{1}{2} s^T \left(\dot{M}_0 - 2C_0 \right) s - \delta\tilde{W}^T\dot{\hat{W}} \\ &= -s^T K_v s + s^T \left(\varsigma + \tilde{d}_s - \xi sat\,(s) \right) \\ &\quad + \tilde{W}^T \left(sh\,(p) - \delta\dot{\hat{W}} \right) \\ &= -s^T K_v s + s^T \left(\varsigma + \tilde{d}_s - \xi sat\,(s) \right) \end{aligned} \tag{40}$$

TABLE 1. The USV's principle physical parameters [39], [40].

Parameter	Value	Parameter	Value
m	23.8	N_r	-1.9
I_{zz}	1.76	$X_{\dot{u}}$	-2.0
X_G	0.046	$Y_{\dot{v}}$	-10.0
X_u	-0.72253	$Y_{\dot{r}}$	-0.1
Y_v	-0.88965	$N_{\dot{v}}$	0
Y_r	-7.25	$N_{\dot{r}}$	-0.1
N_v	0.0313		

where $\tilde{d}_m = d_m - \hat{d}_m = \tilde{W}h(p) + \varsigma$, ξ is selected as: $\xi \geq \varsigma^* + \left\|\tilde{d}_s(0)\right\| + \left\|\frac{\mu}{L}\right\|$.

If $\|s\| \leq \Delta$, then the derivative of V can be calculated as:

$$\begin{aligned}\dot{V} &= -s^T K_v s + s^T\left(\varsigma + \tilde{d}_s\right) - \frac{\xi^2}{4\varepsilon}s^2 \\ &= -s^T K_v s + s^T\left(\varsigma + \tilde{d}_s\right) - \xi\|s\| + \varepsilon \\ &\quad -\left(\frac{1}{2\sqrt{\varepsilon}}\xi\|s\| - \sqrt{\varepsilon}\right)^2 \\ &\leq -s^T K_v s + \|s\|\left(\varsigma^* + \left\|\tilde{d}_s(0)\right\| + \left\|\frac{\mu}{L}\right\| - \xi\right) + \varepsilon \\ &\leq -s^T K_v s + \varepsilon \end{aligned} \tag{41}$$

If $\|s\| > \Delta$, then the derivative of V can be calculated as:

$$\begin{aligned}\dot{V} &= -s^T K_v s - \xi\|s\| + s^T\left(\varsigma + \tilde{d}_s\right) \\ &\leq -s^T K_v s + \left(\|\varsigma\| + \left\|\tilde{d}_s\right\| - \xi\right)\|s\| \\ &\leq -s^T K_v s + \left(\varsigma^* + \left\|\tilde{d}_s(0)\right\| + \left\|\frac{\mu}{L}\right\| - \xi\right)\|s\| \\ &\leq -s^T K_v s \\ &\leq -s^T K_v s + \varepsilon \end{aligned} \tag{42}$$

According to the Lyapunov stability theorem, s, $\tilde{d}_m$, e and $\dot{e}$ are all bounded, the stability of the overall closed-loop USV control system is verified and all the signals are bounded. The proof of *Theorem* is complete.

Remark: With the proposed control design (22), the external disturbances d_s can be well estimated and compensated, and the modeling uncertainties d_m can be well approximated and compensated, thus the good trajectory tracking performance can be achieved.

V. SIMULATION

A. SIMULATION SETUP

To describe and verify the tracking performance of our proposed control algorithm, the benchmark prototype CyberShip II [39], [40] is selected as the platform of our comparative simulation, and the principal physical parameters of this platform are listed in Table 1. All quantities in the simulation are expressed in the international system of units (SI).

To make the trajectory tracking superiority of our control design more convincing, the linear control, PID control, sliding mode control are selected as comparative object of our proposed control design, which can be shown in detail as below:

C1: Linear controller (proposed in [15]). The primary parameters are specified as $k_v = 100$, $k_{c1} = 1$, $k_{c2} = 1$, $d_w = 0.1$, $\tau = 0.1$, $\gamma_u = \gamma_\beta = \gamma_r = 0.01$.

C2: Traditional PID controller. The control law is selected as the following equation:

$$\tau = R(\psi)^T\left(K_p(\eta_d - \eta) + K_d(\dot{\eta}_d - \dot{\eta}) + K_i\int(\eta_d - \eta)\,dt\right) \tag{43}$$

where $K_p = diag\{100, 100, 100\}$, $K_d = diag\{100, 100, 100\}$, $K_i = diag\{20, 20, 20\}$.

C3: Sliding mode controller proposed in [16]. The primary parameters are specified as $K_v = diag\{100, 100, 100\}$, $\xi = diag\{100, 100, 100\}$, $K = diag\{10, 10, 10\}$, $H = diag\{0.1309, 0.1309, 0.1309\}$, $\delta = 0.1$, $\Delta = 0.1$.

C4: Adaptive sliding mode controller using RBFNN and disturbance-observer. The control law, rbfnn approximator and disturbance-observer for the USV are selected as (22), (24) and (31), where $K_v = diag\{100, 100, 100\}$, $\xi = diag\{100, 100, 100\}$, $K = diag\{10, 10, 10\}$, $H = diag\{0.1309, 0.1309, 0.1309\}$, $\delta = 0.1$, $\Delta = 0.1$.

To verify the robustness of these comparative control algorithms, the complex modeling uncertainties d_m can be simulated as: $d_m = \left[\begin{array}{ccc} d_{mx} & d_{my} & d_{m\psi}\end{array}\right]^T$, where

$$d_{mx} = 2\cos(\dot{x}_d) + \sin(x_d) + 2\sin(x - x_d) + 2\cos(\dot{x} - \dot{x}_d) \tag{44}$$

$$d_{my} = 3\cos(\dot{y}_d) + \sin(y_d) + 4\sin(y - y_d) + 2.5\cos(\dot{y} - \dot{y}_d) \tag{45}$$

$$\begin{aligned} d_{m\psi} &= 0.4\cos\left(\dot{\psi}_d\right) + 0.3\sin(\psi_d) + 4\sin(\psi - \psi_d) \\ &\quad + 2\cos\left(\dot{\psi} - \dot{\psi}_d\right) \end{aligned} \tag{46}$$

Moreover, the external disturbances d_s can be simulated as:

$$d_s = \left[\begin{array}{c} 15 + 0.2sin\left(0.1\pi t - \frac{\pi}{3}\right) + 0.3\cos\left(0.3\pi t + \frac{\pi}{4}\right) \\ 17 + 0.3\sin\left(0.2\pi t + \frac{\pi}{4}\right) + 0.4\cos\left(0.1\pi t - \frac{\pi}{6}\right) \\ 7 + 0.5\sin\left(0.3\pi t + \frac{\pi}{6}\right) + 0.15\cos\left(0.2\pi t - \frac{\pi}{3}\right) \end{array}\right] \tag{47}$$

In addition, MIAC index [41] is introduced to evaluate and compare the tracking performance of these comparative control algorithms with the integrate consideration of the transient and steady-state tracking, which is designed as:

$$MIAC = \frac{1}{t_f - t_0}\int_{t_0}^{t_f}|j_e|dt \tag{48}$$

where j_e represents the tracking errors x_e, y_e, ψ_e, t_0 and t_f represent the start simulate time and end simulate time respectively.

As is known to all, the linear controller has good trajectory tracking performance for some specific trajectories at the equilibrium point (13) and not track well for the trajectory which away from the equilibrium point [15]. To verify tracking performance of these comparative control algorithms with different desired trajectories, two simulations are designed as follows, which reflects somewhat practical tracking performance.

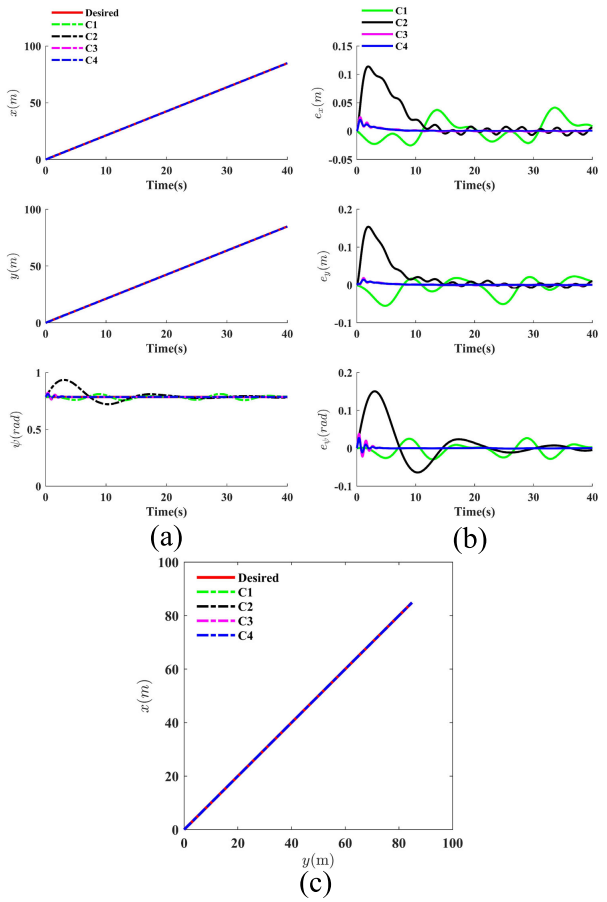

FIGURE 4. The tracking performance of these comparative controllers in SET1.

SET1: Straight-Line Trajectory Tracking
SET2: Circular Trajectory Tracking

B. SIMULATION OF SET1

To compare with the tracking performance of these control algorithms with the physical effect of the specific equilibrium point, the desired trajectory for simulation SET1 is designed as (51)-(52) and Fig.4(c). Simultaneously, the equilibrium point of this desired trajectory is listed as follows:

$$u = 3, v = 0, r = 0, \delta_r = 0, T = 10 \tag{49}$$

$$x_d = \frac{3\sqrt{2}}{2}t 0 \le t \le 40 \tag{50}$$

$$y_d = \frac{3\sqrt{2}}{2}t 0 \le t \le 40 \tag{51}$$

$$\psi_d = \frac{\pi}{4} 0 \le t \le 40 \tag{52}$$

The USV's initial state in SET1 is selected as: $\eta = \left[0\ 0\ \frac{\pi}{4}\right]$, $\dot{\eta} = \left[3\cos\left(\frac{\pi}{4}\right)\ 3\sin\left(\frac{\pi}{4}\right)\ 0\right]$.

With the comparative simulation in SET1, the simulate results are shown in Fig.4-Fig.6. The control input of proposed control is shown in Fig.5. The trajectory tracking performance of USV with these comparative control algorithms is shown in Fig.4(a), which reflects that the desired trajectory

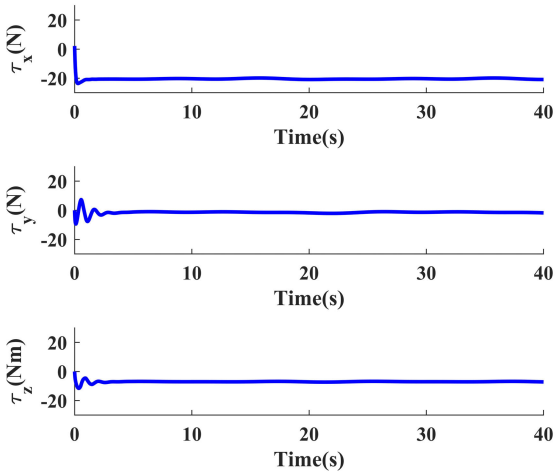

FIGURE 5. The control input of proposed controller in SET1.

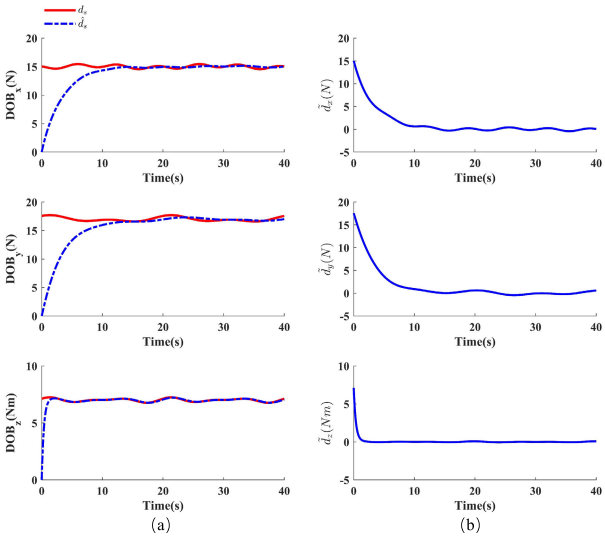

FIGURE 6. The estimate performance of disturbance observer (31) in SET1.

are tracked by the USV accurately and smoothly. Meanwhile, Fig.4(b) shows the corresponding tracking errors, which can be closer converge to a reasonable range gradually. Subsequently, the stability of these comparative control algorithms is verified. Furthermore, to show the control superiority of our control design in detail, the MIAC of different comparative control algorithms in SET1 are listed in table 2. It can be seen that $MIAC_{x_e}$ of C4 is 9.47% of C1, 7.32% of C2 and 81.82% of C3, $MIAC_{y_e}$ of C4 is 6.19% of C1, 5.09% of C2 and 77.78% of C3, $MIAC_{\psi_e}$ of C4 is 7.24% of C1, 3.02% of C2 and 73.33% of C3. Therefore, for the desired trajectory at the equilibrium point, it can be judged that the proposed control design has better performance in terms of transient response and robustness compared with other controllers.

Furthermore, Fig.6(a) shows the estimate performance of observer (31), where the blue line and the red line represent the estimate value of observer (31) and the practical external disturbances respectively. Simultaneously, to show the estimated capacity of the observer (31), the corresponding

TABLE 2. MIAC of these comparatives controllers in SET1.

MIAC	Value
C1:controller proposed in [15]	$MIAC_{x_e} = 0.0190$ $MIAC_{y_e} = 0.0226$ $MIAC_{\psi_e} = 0.0152$
C2:PID controller	$MIAC_{x_e} = 0.0246$ $MIAC_{y_e} = 0.0275$ $MIAC_{\psi_e} = 0.0364$
C3:controller proposed in [16]	$MIAC_{x_e} = 0.0022$ $MIAC_{y_e} = 0.0018$ $MIAC_{\psi_e} = 0.0015$
C4:proposed control design	$MIAC_{x_e} = 0.0018$ $MIAC_{y_e} = 0.0014$ $MIAC_{\psi_e} = 0.0011$

estimate error is shown in Fig.6(b), which can achieve ultimately bounded within a reasonable range gradually. Therefore, the stability and estimate capacity of disturbance observer are verified. Subsequently, the approximate performance of rbfnn approximator (24) is shown in Fig.7(a). The blue line and the red line in Fig.7(a) represent the approximate value of rbfnn (24) and the practical modeling uncertainties respectively. Fig.7(b) describes the corresponding approximate error, which can converge to a reasonable range gradually. Therefore, the stability and approximate capacity of rbfnn approximator (24) are verified.

C. SIMULATION OF SET2

To evaluate and analyze the tracking performance of these comparative control algorithms with the trajectory away from the equilibrium point, the desired trajectory of SET2 is designed as (53)-(55) and Fig.8(c).

$$x_d = \begin{cases} 15 & 0 \le t \le T_1 \\ 15\cos(0.2(t-T_1)) & T_1 < t \le T_2 \\ -15 & T_2 < t \le T_3 \\ -15 & T_3 < t \le T_4 \\ -15\cos(0.2(t-T_4)) & T_4 < t \le T_5 \\ 15 & T_5 < t \le T_6 \end{cases} \tag{53}$$

$$y_d = \begin{cases} 5t - 0.1t^2 & 0 \le t \le T_1 \\ 15\sin(0.2(t-T_1)) + 40 & T_1 < t \le T_2 \\ 40 - 3(t-T_2) - 0.1(t-T_2)^2 & T_2 < t \le T_3 \\ -5t + 0.1(t-T_3)^2 & T_3 < t \le T_4 \\ -15\sin(0.2(t-T_4)) - 40 & T_4 < t \le T_5 \\ 3t + 0.1(t-T_5)^2 - 40 & T_5 < t \le T_6 \end{cases} \tag{54}$$

$$\psi_d = \begin{cases} \frac{\pi}{2} & 0 \le t \le T_1 \\ 0.2(t-T_1) + \frac{\pi}{2} & T_1 < t \le T_2 \\ \frac{3\pi}{2} & T_2 < t \le T_3 \\ \frac{3\pi}{2} & T_3 < t \le T_4 \\ 0.2(t-T_4) + \frac{3\pi}{2} & T_4 < t \le T_5 \\ \frac{5\pi}{2} & T_5 < t \le T_6 \end{cases} \tag{55}$$

where $T_1 = 10$, $T_2 = 10+5\pi$, $T_3 = 20+5\pi$, $T_4 = 30+5\pi$, $T_5 = 30+10\pi$, $T_6 = 40+10\pi$. The USV's initial state in SET2 is selected as: $\eta = \left[\begin{array}{ccc} 15 & 0 & \frac{\pi}{2} \end{array}\right]$, $\dot{\eta} = \left[\begin{array}{ccc} 0 & 5 & 0 \end{array}\right]$.

With the comparative simulation in SET2, the corresponding results are shown in Fig.8-Fig.10. The control input of

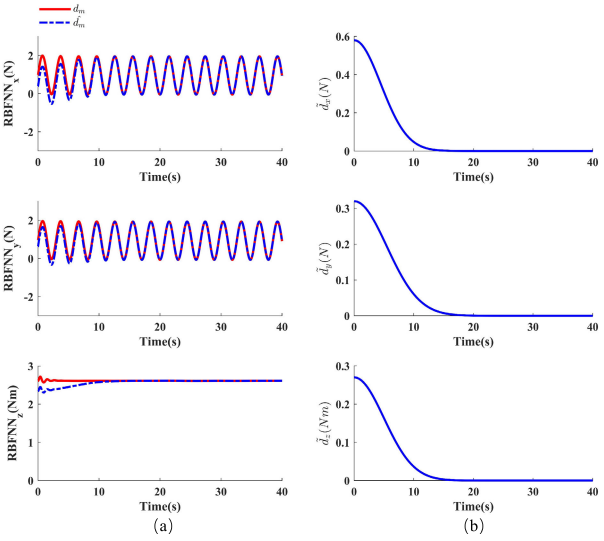

FIGURE 7. The approximate performance of rbfnn (24) in SET1.

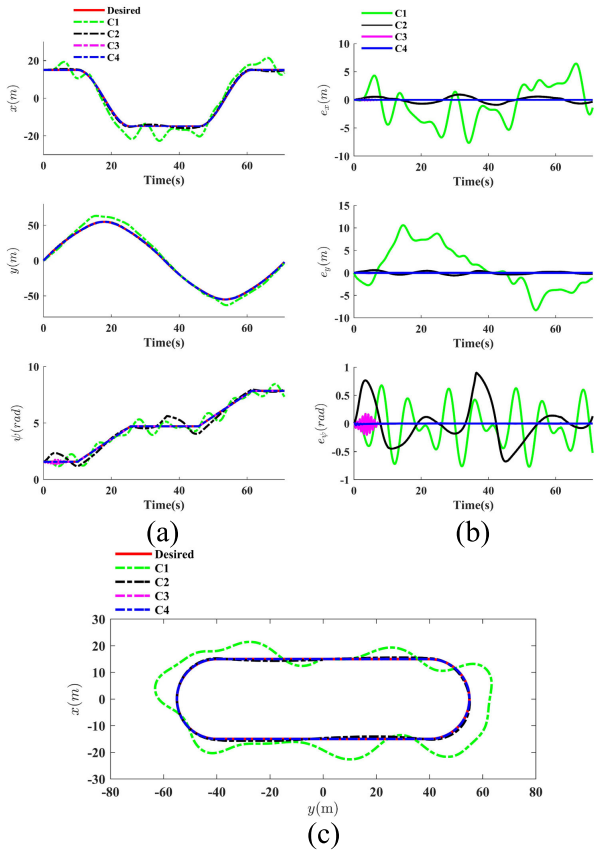

FIGURE 8. The tracking performance of these comparative controllers in SET2.

proposed control is shown in Fig.9. The trajectory tracking performance is shown in Fig.8(a), and corresponding tracking error e is shown in Fig.8(b). It can be derived from above results that the corresponding tracking error e of C1 and C2, approximator error $\tilde{d}_m$ and estimate error $\tilde{d}_s$ can converge to a small reasonable range gradually, which verifies the stability

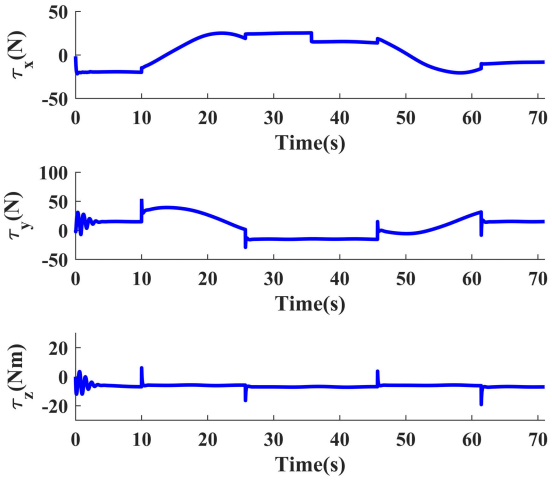

FIGURE 9. The control input of proposed controller in SET2.

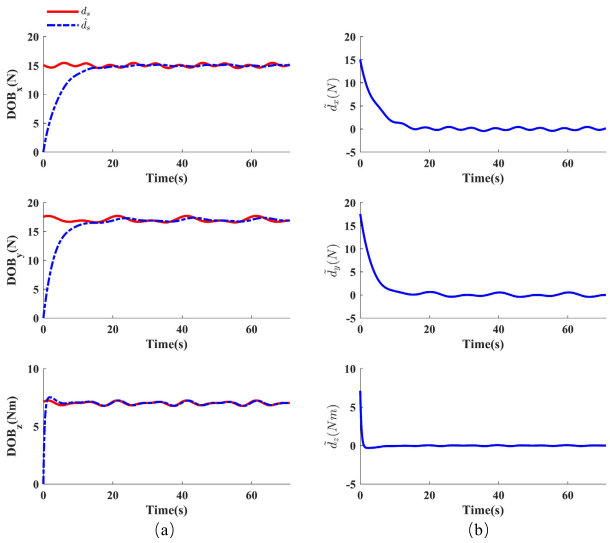

FIGURE 10. The estimate performance of disturbance observer (31) in SET2.

and effectiveness of PID controller and proposed control design. It is worth noting that the tracking error e of C3 is larger than C1 and C2 evidently, which reflects that the linear controller is not suitable for the USV's tracking with the desired trajectory away from the equilibrium point. Table 3 shows the MIAC in SET2, which can be calculated that $MIAC_{x_e}$ of C4 is 0.013% of C1, 0.082% of C2 and 10% of C3, $MIAC_{y_e}$ of C4 is 0.022% of C1, 0.318% of C2 and 41.3% of C3, $MIAC_{\psi_e}$ of C4 is 0.48% of C1, 0.49% of C2 and 15.1% of C3. Therefore, according to the abovementioned comparison, with the desired trajectory away from the equilibrium point, the proposed control design has better performance in terms of transient response and robustness than other comparative controllers.

According to the above analysis of simulate results in SET1 and SET2, compared with linear controller C1, PID controller C2 and sliding mode controller C3, the tracking priority and effectiveness of proposed control design are verified.

TABLE 3. MIAC of these comparative controllers in SET2.

MIAC	Value
C1:controller proposed in [15]	$MIAC_{x_e} = 6.3337$ $MIAC_{y_e} = 8.7876$ $MIAC_{\psi_e} = 0.6626$
C2:PID controller	$MIAC_{x_e} = 0.9712$ $MIAC_{y_e} = 0.5976$ $MIAC_{\psi_e} = 0.5893$
C3:controller proposed in [16]	$MIAC_{x_e} = 0.0080$ $MIAC_{y_e} = 0.0046$ $MIAC_{\psi_e} = 0.0192$
C4:proposed control design	$MIAC_{x_e} = 0.0008$ $MIAC_{y_e} = 0.0019$ $MIAC_{\psi_e} = 0.0029$

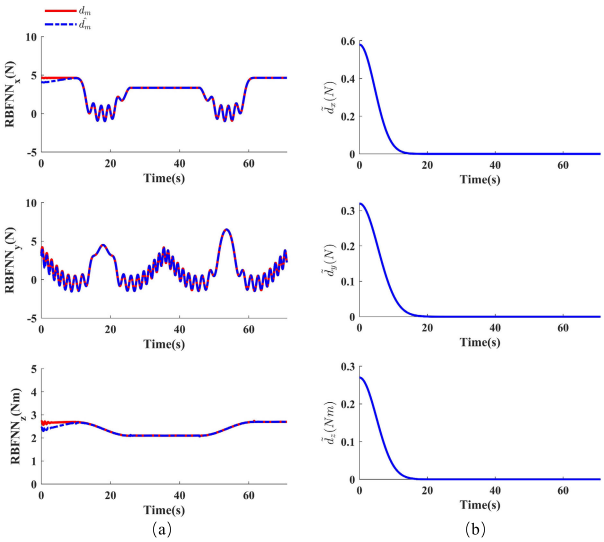

FIGURE 11. The approximate performance of rbfnn (24) in SET2.

VI. CONCLUSION

An adaptive sliding mode control design using RBFNN and disturbance-observer is proposed in this paper for nonlinear USV system with modeling uncertainties (e.g., modeling error and parameter variations) and external disturbances (wind, wave, current, etc). Firstly, a nonlinear dynamic model is derived in detail with full account of modeling uncertainties and external disturbance. Subsequently, a RBFNN approximator is designed to approximate and compensate modeling uncertainties, and a disturbance-observer is developed to estimate and compensate the external disturbance. Based on the RBFNN approximator and disturbance-observer, a slide-mode controller is developed to track any kinds of desired trajectories. Thus, the integrated effect of nonlinearities, modeling uncertainties and external disturbances for the USV's trajectory tracking can be well handled. Moreover, the overall stability of the closed-loop control system is strictly guaranteed. A set of comparative simulations are implemented and MIAC is calculated simultaneously to analyze the tracking performance. The simulate results verify the significant priority of our proposed control design with faster response, better transient and robustness. In the future, we will consider the impact of control input saturation, violent external

disturbances and modeling uncertainties on system robust stability and tracking performance. Furthermore, the proposed control design will be applied for the practical experiments, and corresponding experimental results will be analyzed.

REFERENCES

[1] Z. Dong, L. Wan, Y. Li, T. Liu, and G. Zhang, "Trajectory tracking control of underactuated USV based on modified backstepping approach," *Int. J. Nav. Archit. Ocean Eng.*, vol. 7, pp. 817–832, 2015.
[2] Z. Chen, B. Yao, and Q. Wang, "μ-synthesis-based adaptive robust control of linear motor driven stages with high-frequency dynamics: A case study," *IEEE/ASME Trans. Mechatronics*, vol. 20, no. 3, pp. 1482–1490, Jun. 2015.
[3] C. Li, C. Li, Z. Chen, and B. Yao, "Advanced synchronization control of a dual-linear-motor-driven gantry with rotational dynamics," *IEEE Trans. Ind. Electron.*, vol. 65, no. 9, pp. 7526–7535, Sep. 2018.
[4] Z. Chen, F. Huang, W. Sun, J. Gu, and B. Yao, "RBF neural network based adaptive robust control for nonlinear bilateral teleoperation manipulators with uncertainty and time delay," *IEEE/ASME Trans. Mechatronics*, to be published, doi: 10.1109/TMECH.2019.2962081.
[5] Z. Chen, Y. Zhang, Y. Zhang, Y. Nie, J. Tang, and S. Zhu, "A hybrid path planning algorithm for unmanned surface vehicles in complex environment with dynamic obstacles," *IEEE Access*, vol. 7, pp. 126439–126449, 2019.
[6] X. Sun, G. Wang, Y. Fan, D. Mu, and B. Qiu, "Collision avoidance of podded propulsion unmanned surface vehicle with COLREGs compliance and its modeling and identification," *IEEE Access*, vol. 6, pp. 55473–55491, 2018.
[7] D. D. Mu, Y. S. Zhao, and G. F. Wang, "Course control of USV based on fuzzy adaptive guide control," in *Proc. Chin. Control Decis. Conf. (CCDC)*, May 2016, pp. 6433–6437.
[8] Z. Liu, Y. Zhang, X. Yu, and C. Yuan, "Unmanned surface vehicles: An overview of developments and challenges," *Annu. Rev. Control*, vol. 41, pp. 71–93, May 2016.
[9] Y. Liu and R. Bucknall, "Efficient multi-task allocation and path planning for unmanned surface vehicle in support of ocean operations," *Neurocomputing*, vol. 275, pp. 1550–1566, Jan. 2018.
[10] Y.-L. Wang and Q.-L. Han, "Network-based fault detection filter and controller coordinated design for unmanned surface vehicles in network environments," *IEEE Trans Ind. Informat.*, vol. 12, no. 5, pp. 1753–1765, Oct. 2016.
[11] D. D. Mu, G. F. Wang, and Y. S. Fan, "Design of adaptive neural tracking controller for pod propulsion unmanned vessel subject to unknown dynamics," *J. Elect. Eng. Technol.*, vol. 12, no. 6, pp. 2365–2377, 2017.
[12] B. Qiu, G. Wang, Y. Fan, D. Mu, and X. Sun, "Adaptive course control-based trajectory linearization control for uncertain unmanned surface vehicle under rudder saturation," *IEEE Access*, vol. 7, pp. 108768–108780, 2019.
[13] N. Wang, Z. Sun, J. Yin, S.-F. Su, and S. Sharma, "Finite-time observer based guidance and control of underactuated surface vehicles with unknown sideslip angles and disturbances," *IEEE Access*, vol. 6, pp. 14059–14070, 2018.
[14] N. Wang, Z. Sun, J. Yin, Z. Zou, and S.-F. Su, "Fuzzy unknown observer-based robust adaptive path following control of underactuated surface vehicles subject to multiple unknowns," *Ocean Eng.*, vol. 176, pp. 57–64, Mar. 2019.
[15] J. Shin, D. J. Kwak, and Y.-I. Lee, "Adaptive path-following control for an unmanned surface vessel using an identified dynamic model," *IEEE/ASME Trans. Mechatronics*, vol. 22, no. 3, pp. 1143–1153, Jun. 2017.
[16] Z. Chen, Y. Zhang, Y. Zhang, Y. Nie, J. Tang, and S. Zhu, "Disturbance-observer-based sliding mode control design for nonlinear unmanned surface vessel with uncertainties," *IEEE Access*, vol. 7, pp. 148522–148530, 2019.
[17] N. Wang, J.-C. Sun, M. J. Er, and Y.-C. Liu, "A novel extreme learning control framework of unmanned surface vehicles," *IEEE Trans. Cybern.*, vol. 46, no. 5, pp. 1106–1117, May 2016.
[18] T. Liu, Z. Dong, H. Du, L. Song, and Y. Mao, "Path following control of the underactuated USV based on the improved Line-of-Sight guidance algorithm," *Polish Maritime Res.*, vol. 24, no. 1, pp. 3–11, Mar. 2017.
[19] Y.-L. Liao, M.-J. Zhang, L. Wan, and Y. Li, "Trajectory tracking control for underactuated unmanned surface vehicles with dynamic uncertainties," *J. Central South Univ.*, vol. 23, no. 2, pp. 370–378, Feb. 2016.
[20] A. S. K. Annamalai, R. Sutton, C. Yang, P. Culverhouse, and S. Sharma, "Robust adaptive control of an uninhabited surface vehicle," *J. Intell. Robotic Syst.*, vol. 78, no. 2, pp. 319–338, 2015.
[21] Y.-L. Wang and Q.-L. Han, "Network-based heading control and rudder oscillation reduction for unmanned surface vehicles," *IEEE Trans. Control Syst. Technol.*, vol. 25, no. 5, pp. 1609–1620, Sep. 2017.
[22] J. Hu, H. Zhang, X. Yu, H. Liu, and D. Chen, "Design of sliding-mode-based control for nonlinear systems with mixed-delays and packet losses under uncertain missing probability," *IEEE Trans. Syst., Man, Cybern. Syst.*, pp. 1–12, 2019.
[23] H. Zhang, J. Hu, and X. Yu, "Adaptive sliding mode fault-tolerant control for a class of uncertain systems with probabilistic random delays," *IEEE Access*, vol. 7, pp. 64234–64246, 2019.
[24] J. Han, J. Xiong, Y. He, F. Gu, and D. Li, "Nonlinear modeling for a water-jet propulsion USV: An experimental study," *IEEE Trans. Ind. Electron.*, vol. 64, no. 4, pp. 3348–3358, Apr. 2017.
[25] L. Chen, R. Cui, C. Yang, and W. Yan, "Adaptive neural network control of underactuated surface vessels with guaranteed transient performance: Theory and experimental results," *IEEE Trans. Ind. Electron.*, vol. 67, no. 5, pp. 4024–4035, May 2020, doi: 10.1109/TIE.2019.2914631.
[26] G. Guo and P. Zhang, "Asymptotic stabilization of USVs with actuator dead-zones and yaw constraints based on fixed-time disturbance observer," *IEEE Trans. Veh. Technol.*, vol. 69, no. 1, pp. 302–316, Jan. 2020.
[27] Y. Deng, X. Zhang, N. Im, G. Zhang, and Q. Zhang, "Model-based event-triggered tracking control of underactuated surface vessels with minimum learning parameters," *IEEE Trans. Neural Netw. Learn. Syst.*, to be published, doi: 10.1109/TNNLS.2019.2951709.
[28] Y. Tan, G. Cai, B. Li, K. L. Teo, and S. Wang, "Stochastic model predictive control for the set point tracking of unmanned surface vehicles," *IEEE Access*, vol. 8, pp. 579–588, 2020.
[29] C. Lv, H. Yu, J. Chi, T. Xu, H. Zang, H. L. Jiang, and Z. Zhang, "A hybrid coordination controller for speed and heading control of underactuated unmanned surface vehicles system," *Ocean Eng.*, vol. 176, pp. 222–230, Mar. 2019.
[30] F. Huang, W. Zhang, Z. Chen, J. Tang, W. Song, and S. Zhu, "RBFNN-based adaptive sliding mode control design for nonlinear bilateral teleoperation system under time-varying delays," *IEEE Access*, vol. 7, pp. 11905–11912, 2019.
[31] Z. Chen, B. Yao, and Q. Wang, "Accurate motion control of linear motors with adaptive robust compensation of nonlinear electromagnetic field effect," *IEEE/ASME Trans. Mechatronics*, vol. 18, no. 3, pp. 1122–1129, Jun. 2013.
[32] Z. Chen, C. Li, B. Yao, M. Yuan, and C. Yang, "Integrated coordinated/synchronized contouring control of a dual-linear-motor-driven gantry," *IEEE Trans. Ind. Electron.*, vol. 67, no. 5, pp. 3944–3954, May 2020.
[33] Z. Chen, F. Huang, C. Yang, and B. Yao, "Adaptive fuzzy backstepping control for stable nonlinear bilateral teleoperation manipulators with enhanced transparency performance," *IEEE Trans. Ind. Electron.*, vol. 67, no. 1, pp. 746–756, Jan. 2020.
[34] Z. Chen, F. Huang, W. Chen, J. Zhang, W. Sun, J. Chen, J. Gu, and S. Zhu, "RBFNN-based adaptive sliding mode control design for delayed nonlinear multilateral telerobotic system with cooperative manipulation," *IEEE Trans Ind. Informat.*, vol. 16, no. 2, pp. 1236–1247, Feb. 2020.
[35] W. Sun, J. Zhang, and Z. Liu, "Two-Time-Scale redesign for antilock braking systems of ground vehicles," *IEEE Trans. Ind. Electron.*, vol. 66, no. 6, pp. 4577–4586, Jun. 2019.
[36] W. Sun, Y. Liu, and H. Gao, "Constrained sampled-data ARC for a class of cascaded nonlinear systems with applications to motor-servo systems," *IEEE Trans Ind. Informat.*, vol. 15, no. 2, pp. 766–776, Feb. 2019.
[37] J. Yao and W. Deng, "Active disturbance rejection adaptive control of hydraulic servo systems," *IEEE Trans. Ind. Electron.*, vol. 64, no. 10, pp. 8023–8032, Oct. 2017.
[38] J. Yao, W. Deng, and Z. Jiao, "RISE-based adaptive control of hydraulic systems with asymptotic tracking," *IEEE Trans. Autom. Sci. Eng.*, vol. 14, no. 3, pp. 1524–1531, Jul. 2017.
[39] N. Wang, S.-F. Su, X. Pan, X. Yu, and G. Xie, "Yaw-guided trajectory tracking control of an asymmetric underactuated surface vehicle," *IEEE Trans Ind. Informat.*, vol. 15, no. 6, pp. 3502–3513, Jun. 2019.
[40] R. Skjetne, "The maneuvering problem," Ph.D. dissertation, Dept. Eng. Cybern., Norwegian Univ., Sci. Technol., Trondheim, Norway, 2005.
[41] G. Zhu and J. Du, "Global robust adaptive trajectory tracking control for surface ships under input saturation," *IEEE J. Ocean. Eng.*, to be published, doi: 10.1109/JOE.2018.2877895.

ZHENG CHEN (Senior Member, IEEE) received the B.Eng. and Ph.D. degrees in mechatronic control engineering from Zhejiang University, Zhejiang, China, in 2007 and 2012, respectively.

From 2013 to 2015, he was a Postdoctoral Researcher with the Department of Mechanical Engineering, Dalhousie University, Halifax, NS, Canada. Since 2015, he has been an Associate Professor with the Ocean College, Zhejiang University. His research interests mainly focus on advanced control of robotic and mechatronic systems, such as nonlinear adaptive robust control, motion control, trajectory planning, telerobotics, exoskeleton, mobile manipulator, precision mechatronic systems, and underwater robot.

YOUGONG ZHANG received the B.Eng. degree in mechanical engineering from Nanchang University, Jiangxi, China, in 2018. He is currently pursuing the M.Eng. degree with the Ocean College, Zhejiang University.

His research interest includes control of robotics.

YONG NIE received the Ph.D. degree in mechatronic engineering from Zhejiang University, Zhejiang, China, in 2010.

He is currently a Lecturer with the Department of Mechanical Engineering, Zhejiang University. His research interests include mechatronics system control and simulator.

JIANZHONG TANG received the Ph.D. degree in mechatronic control engineering from Zhejiang University, Zhejiang, China, in 2007.

He is currently an Associate Professor with the Department of Mechanical Engineering, Zhejiang University. His research interests include robotics and mechatronics.

SHIQIANG ZHU received the B.Eng. degree in mechanical engineering from Zhejiang University, Hangzhou, China, in 1988, the M.Eng. degree in mechatronic engineering from the Beijing Institute of Technology, in 1991, and the Ph.D. degree in mechanical engineering from Zhejiang University, in 1995.

He has been a Faculty Member with Zhejiang University, since 1995, where he was promoted to the rank of a Professor, in 2001. He is currently with the Ocean College, Zhejiang University. His research interests include robotics and mechatronics.